



Published in final edited form as:

*Acc Chem Res.* 2021 February 02; 54(3): 605–617. doi:10.1021/acs.accounts.0c00821.

## Ideality in Context: Motivations for Total Synthesis

David S. Peters<sup>‡</sup>, Cody Ross Pitts<sup>‡</sup>, Kyle S. McClymont, Thomas P. Stratton, Cheng Bi, Phil S. Baran

Department of Chemistry, The Scripps Research Institute, La Jolla, California 92037, United States

### CONSPECTUS:

Total synthesis—the ultimate proving ground for the invention and field-testing of new methods, exploration of disruptive strategies, final structure confirmation, and empowerment of medicinal chemistry on natural products—is one of the oldest and most enduring subfields of organic chemistry. In the early days of this field, its sole emphasis focused on debunking the concept of vitalism, that living organisms could create forms of matter accessible only to them. Emphasis then turned to the use of synthesis to degrade and reconstitute natural products to establish structure and answer questions about biosynthesis. It then evolved to not only an intricate science but also a celebrated form of art. As the field progressed, a more orderly and logical approach emerged that served to standardize the process. These developments even opened up the possibility of computer-aided design using retrosynthetic analysis. Finally, the elevation of this field to even higher levels of sophistication showed that it was feasible to synthesize any natural product, regardless of complexity, in a laboratory. During this remarkable evolution, as has been reviewed elsewhere, many of the principles and methods of organic synthesis were refined and galvanized. In the modern era, students and practitioners are still magnetically attracted to this field due to the excitement of the journey, the exhilaration of creation, and the opportunity to invent solutions to challenges that still persist. Contemporary total synthesis is less concerned with demonstrating a proof of concept or a feasible approach but rather aims for increased efficiency, scalability, and even “ideality.” In general, the molecules of Nature are created biosynthetically with levels of practicality that are still unimaginable using the tools of modern synthesis. Thus, as the community strives to do more with less (i.e., innovation), total synthesis is now focused on a pursuit for simplicity rather than a competition for maximal complexity. In doing so, the practitioner must devise outside-the-box strategies supplemented with forgotten or newly invented methods to reduce step count and increase the overall economy of the approach. The downstream applications of this pursuit not only empower students who often go on to apply these skills in the private sector but also lead to new discoveries that can impact numerous disciplines of societal importance. This account traces some select case studies from our laboratory over the past five years that vividly demonstrate our own motivation for dedicating so much effort to this classic field. In aiming for simplicity, we focus on the elusive goal of achieving ideality, a term that, when

---

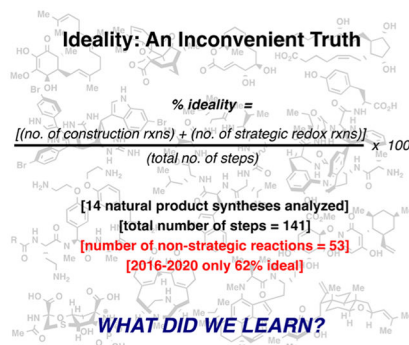
**Corresponding Author: Phil S. Baran** – Department of Chemistry, The Scripps Research Institute, La Jolla, California 92037, United States; pbaran@scripps.edu.

<sup>‡</sup>D.S.P. and C.R.P. contributed equally.

The authors declare no competing financial interest.

taken in the proper context, can serve as a guiding light to point the way to furthering progress in organic synthesis.

## Graphical Abstract



## INTRODUCTION

The term “ideality” in the context of organic chemistry was introduced in 2010 to pinpoint flaws in a synthetic sequence.<sup>2</sup> Inspired by Hendrickson’s seminal studies on efficiency in synthesis it simply states that in order for a synthesis to be *ideal*, it must only create skeletal bonds of a molecule without recourse to extraneous functional group manipulations, protecting group sequences, or nonstrategic redox fluctuations (concession steps).<sup>4</sup> Calculating ideality is rather elementary: the total number of strategic steps is divided by the total step count. Like any singular metric that characterizes a synthesis (yield, step count, atom economy), ideality does not tell the whole story. For example, a two-step synthesis where the first step generates all of the key skeletal bonds followed by a deprotection would only be 50% ideal but clearly superior to a 10-step approach with 80% ideality.<sup>5</sup> Similarly, in certain cases it might be valuable to introduce protecting groups or additional steps to aid purification on a large scale. It thus represents an inconvenient truth as even the two-step synthesis mentioned above could be improved. Syntheses are best judged using not only ideality but also by considering step-count,<sup>6</sup> atom-economy,<sup>7</sup> redox-economy,<sup>8</sup> overall yield, convergence,<sup>9</sup> number of isolated intermediates,<sup>10</sup> and, most importantly, the context. For example, on process scale, although ideality has been used for route scouting,<sup>11</sup> various descriptors for overall efficiency that even take into account the quantity of solvent usage are of critical importance (e.g., process mass intensity).<sup>12</sup> In radio-chemistry, most of the above variables do not apply as convergency, time, and cost of the radiolabeled element matter most.<sup>13</sup> In medicinal or discovery chemistry, the ability to divergently and quickly access multiple vectors of SAR space from a common intermediate is usually more important than overall step count.<sup>13</sup> In an academic setting, particularly in natural product synthesis, ideality can be a useful rubric to employ not only at the planning stages and execution, but also in a final analysis when the synthesis is complete. Figure 1 outlines natural product syntheses that our laboratory has completed over the past five years (2016–2020) along with a minimalist retrosynthetic depiction. This account will dive into the motivations for pursuing most of these molecules, what was learned as a consequence, and the lessons of reflecting on the ideality of the final routes (these lessons will be highlighted in bold at the

end of each section). The syntheses are graphically illustrated to highlight key reactions and the strategic (blue) or nonstrategic (red) nature of the steps employed. Natural products that leverage two-phase terpene synthesis (phorbol, thapsigargin, and Taxol) will not be covered here as the logic underlying those syntheses has been reviewed elsewhere.<sup>14</sup>

## 2016

Antroquinonol A (**3**)<sup>15</sup> is a natural product of mixed biosynthetic origin, containing a polyketide-derived quinone portion coupled to a linear diterpene fragment (Figure 2). It was brought to our attention as a target of interest by medicinal chemists at Bristol-Myers-Squibb due to its remarkable anticancer activity.<sup>16</sup> In fact, it was granted orphan drug status by the FDA for treatment of pancreatic cancer and acute myeloid leukemia. Multiple phase II studies promoted the use of **3** in a wide range of indications from Alzheimer's disease and atopic dermatitis to the treatment of COVID-19.<sup>17</sup> As the mechanism of action for **3** was (and still is to our knowledge) unknown, a modular and scalable synthetic strategy was devised commencing from inexpensive benzaldehyde derivative **1**. The key step involved enantiocontrolled vicinal difunctionalization of quinone **2** by enlisting an organocuprate addition, followed by alkylation with farnesyl bromide. Upon stereocontrolled reduction to install the remaining hydroxyl group, deprotection led to gram quantities of **3**. With copious quantities in hand, a barrage of biological assays (*in vitro* and *in vivo*) revealed no appreciable cytotoxic activity. It was thus concluded that the enthusiasm associated with initial findings might be due to an impurity in the natural product isolation process rather than **3** itself. The continued use of **3** in clinical trials remains an enigma. Even so, this six-step synthesis achieved all of the goals set forth at the outset in that it provided ample material for extensive biological tests and offered a roadmap for the synthesis of analogs (although this turned out to be unnecessary). **However, the 50% ideality points to key problems still remaining in synthesis such as the difficulty in chemoselective manipulation of quinones in their native form.**

In contrast to the motivations guiding the synthesis of **3**, the pursuit of the plant-derived natural products pallambins (**8a** and **8b**) was motivated solely on the basis of structural beauty (Figure 2).<sup>18</sup> The retrosynthetic analysis was predicated on the notion that four sequential cyclization/annulation events could consecutively form each ring system. This carefully choreographed sequence, beginning with furfuryl alcohol **4**, commenced with a tandem Eschenmoser—Claisen/reduction followed by a Robinson annulation and vicinal difunctionalization to furnish enol ether **5**. The furan served as a masked 1,4-dicarbonyl compound that could be strategically unveiled, thus setting the stage for the next cyclization delivering **6**. A nonstrategic debromination followed by desaturation and elimination provided furan **7**. The final sequence accomplished a formal annulation forging both C—C and C—O bonds of the  $\gamma$ -lactone that could be immediately subjected to an aldol reaction with acetaldehyde to deliver **8a** and **8b**. While the ideality of this route is high, it is not without warts. For example, **the route is linear in nature and one could imagine reducing the step count if a more convergent approach were devised.** Additionally, although the use of a furan to shield a 1,4-dicarbonyl group is an often-used tactic<sup>19</sup> and does put in place the needed functionality for the ensuing cyclization, it is debatable whether such a sequence is truly strategic. An even more direct approach would involve the cyclization (perhaps

through SET oxidation) of the enol ether and furan groups in **5** to deliver a nonbrominated structure analogous to **6**, perhaps obviating the need for nonstrategic debromination and elimination steps.

In the case of maoecrystal V (**14**),<sup>20</sup> a popular plant-derived natural product target, the goal was to develop a scalable route to address the unanswered questions surrounding its reported anticancer activity (Figure 2).<sup>21</sup> In stark departure from four prior approaches that were all wedded to intuitive Diels—Alder disconnections,<sup>22</sup> a convergent approach loosely mirrored on the proposed biosynthesis<sup>23</sup> was chosen that, on paper, would dramatically simplify and shorten the route. Thus, fragment **10**, derived from cyclohexenone **9** via enantioselective conjugate addition and intramolecular Sakurai cyclization, was merged with enone **11** to generate the key C—C bond linkage, which upon heating with PTSA smoothly afforded key intermediate **12** after a pinacol rearrangement. Although this was a powerfully short entry to the synthesis, extensive optimization was required to install the remaining two carbon atoms, the proper stereochemistry, and the requisite oxidation state found in the natural product. This was accomplished through the following carefully choreographed sequence involving: (1) a La-directed, site-selective, and stereocontrolled aldol with formaldehyde, (2) a Zn-assisted stereoselective ketone reduction, (3) a strategic hemiketal formation followed by stereoselective cyanide addition, and (4) a cascade oxidation sequence to install the enone in **14**. Ultimately, with a copious supply of **14** in hand we were able to conclude, as with antroquinonol (*vide supra*), that the initial enthusiasm associated with the differential cytotoxicity reported for **14** was likely due to an impurity in the initial isolate. Although the ideality of this route was high (73%), **it suffered from two protecting group manipulations and an extraneous redox fluctuation**. These concession steps were required to set the stage for the fragment union and pinacol shift, and use of a DNB protecting group stemmed from a need to prevent the wrong hemiketal from forming.

Our longstanding interest in the marine-derived pyrroleimidazole alkaloids<sup>24</sup> inspired investigation into a conceptually related family of alkaloids bearing a striking set of repeating indole-imidazole subunits called the araiosamines (Figure 2).<sup>25</sup> The synthetic challenge posed by these exotic polycyclic architectures was the sole justification for their pursuit in our laboratory. A hypothesis driving our key retrosynthetic disconnections was that their complex structures could be unraveled by invoking a thermodynamic cyclization of a suitably functionalized guanidine-containing indole trimer dubbed *prearaiosamine* **21**.<sup>26</sup> While initial studies on ambitious cascade trimerizations of indole-based building blocks failed, a more stepwise approach ultimately proved successful. The construction of the requisite indole trimer **19** could be accomplished using Mannich and aldol reactions with three simple building blocks: an imine derived from **15**, nitrile **16**, and ester **17**. This enabled clean differentiation of the requisite functionality necessary for installing guanidines at key positions. A particularly recalcitrant guanidine installation required the invention of a new reagent for this purpose (**18**, currently sold by Millipore-Sigma as “TurboGuan”). Subsequent adjustment of the ester oxidation state, setting the remaining amino stereocenter, and appending the second guanidine unit arrived at a functional precursor to *prearaiosamine*, **20**. Finally, submission of this precursor to PPTS in warm water led to targets **22a** and **22b** presumably by way of a thermodynamic equilibration. Ironically, biological

evaluation of the natural products revealed interesting antibacterial activity despite original reports to the contrary, unlike the seemingly promising isolation studies on **3** and **14**. The complexity of the target and its challenging physical properties resulted in a route with only 64% ideality, and while not mentioned above, the stereoselectivity of certain steps was also low (1:1) despite extensive optimization. **If trimerization of the simple indole building blocks could be achieved in a controllable fashion, most of the issues of this synthesis could be resolved. This points to unresolved chemical challenges in aldol/Mannich chemistry that Nature has mastered.**

## 2017

Our interests in large peptidic macrocyclic natural products such as lugdunin<sup>27</sup> (**24**) stemmed from a long-term collaboration with Bristol-Myers-Squibb (Figure 3). Traditionally, macrocyclization strategies to access native cyclic peptides utilize kinetic, irreversible amide bond-forming methods; the premise of this work was to explore a thermodynamic approach. The existence of macrocyclic peptides bearing imines (or derivatives thereof, e.g. **24**) inspired an exploration into an imine-based macrocyclization pathway.<sup>28</sup> This approach enabled the rapid synthesis of linear amino-aldehyde precursors that upon exposure to a buffered aqueous solution and suitable trap yielded a thermodynamic product via an imine intermediate.<sup>27</sup> Studies demonstrated that preorganization of the linear precursors played no role in the final product formation. In other analogues, one could also see striking selectivity for the *N*-terminus versus adjacent unprotected lysine residues. To demonstrate the value of the approach, a short total synthesis of **24** from **23** was achieved via solid-phase peptide synthesis (SPPS) using a resin-bound hemiaminal followed by tandem cleavage/cyclization. Notably, **24** attracted worldwide interest due to its striking antibacterial activity and origin from the human microbiome.<sup>29</sup> **Clearly the route benefits from the industrialization of SPPS that makes peptide synthesis so routine. Yet, from an ideality standpoint (43%), one cannot ignore the incessant protecting group manipulations that are required to facilitate such sequences.** An interesting challenge for the field, one that has seen some recent progress,<sup>30</sup> would be to reduce the reliance on these concessions.

The cladospolides **29a** and **29b** are polyketide-derived natural products that bear a distinct diol motif (Figure 3). Although 1,2-diols traditionally call for a dihydroxylation transform, an alternative strategy was sought. Tartaric acid has historically been used as a diol “cassette” by way of laborious reduction—oxidation-Wittig sequences that often suffer from a lack of geometric control of the olefin product. For example, a prior route to **29** utilized an 18-step sequence where the desired olefin geometry was not controlled, leading to product mixtures and reduced yield.<sup>31</sup> Our interest in radical retrosynthesis<sup>32</sup> triggered a direct disconnection of the C—CO<sub>2</sub>H bond in tartaric acid to controllably replace it with a geometrically defined alkene-based nucleophile via decarboxylative alkenylation.<sup>33</sup> Sequential use of this cross-coupling on one of the carboxylate moieties, with a decarboxylative alkylation on the other, could allow for a modular approach to a myriad of diol-containing structures. In fact, such an approach accessed cladospolides B **29a** and C **29b** from the chiral pool derived L- and D-tartrate esters **25b** and **25a**, respectively. Thus, commercially available tartrate **25a** was submitted to two sequential decarboxylative

couplings with alkyl zinc **26** and vinyl zinc **27** to afford protected *sec*-ester **28** and intercepting, in 6 steps (LLS), the prior 14-step route.<sup>31</sup> **Despite the brevity of this approach, some concession steps were required, namely the use of protecting group manipulations to facilitate the modular nature of this sequence, resulting in a modest ideality score of 43%.** Some protecting groups could conceivably be excised (e.g., TBS); however, many of those employed were tactical, and function beyond their ability to block the reactivity of a functional group. For example, the acetonide locks the diol ring conformation to enable diastereoselective coupling, while ester hydrolysis allows for iterative control of the cross-coupling steps.

The prostaglandins, a storied class of molecules, have remained popular targets for the synthetic community.<sup>34</sup> PGF<sub>2α</sub> **34** is among the family's most notable members and has several important medical applications (Figure 3). The retrosynthetic analysis toward PGF<sub>2α</sub>, as with **29a** and **29b**, involved iterative scission of its two side chains: alkyl fragment **31** and alkene **33**, tracing back to the commercially available Corey lactone **30**.<sup>35</sup> This disconnection enabled the modular assembly of PGF<sub>2α</sub> in four steps with 50% ideality via decarboxylative alkyl and alkenyl cross-couplings, thus leveraging functionality native to **30**. While the initial redox manipulation and hydrolysis/TBS protection step are nonideal, they are counterbalanced by the brevity of the route, which carries the potential to access innumerable medicinally relevant analogues of PGF<sub>2α</sub> via simple cross-coupling. It is worth reiterating that in the syntheses of **29a**, **29b**, and **34**, one is not wedded to the strict rules for controlling olefin geometry in classic reactions (e.g., Wittig olefination) during the retrosynthetic plan since it is programmed by way of cross-coupling. **That said, the above routes still illustrate how far we have to go when it comes to controlling chemoselectivity without resorting to protecting group chemistry.**

## 2018

The arylomycins<sup>36</sup> are an old class of natural product antibiotics that regained notoriety in 2008 stemming from seminal findings from the Romesberg group<sup>37</sup> that served as a basis for further development at Genentech (Figure 4).<sup>38</sup> Upon our entry into the area, only one macrocyclization strategy, intramolecular Suzuki coupling,<sup>37a,39</sup> was available to forge the key macrocyclic core **38**; however, this route was lengthy (14 steps) and posed problems of material throughput (6.4% overall yield, 36% ideality) in the ongoing medicinal chemistry campaigns (RQx and Genentech).

This key building block not only represented a formal synthesis of **39**<sup>39</sup> (Figure 1) but was a gateway to a wide variety of analogs. Due to its peptidic nature, our retrosynthetic analysis was predicated on the use of amino acid building blocks and, by mimicking biosynthesis, necessitated the use of C-H functionalization logic to obviate concession steps associated with prefunctionalization of the phenolic building blocks. This allowed a simple unfunctionalized tripeptide **37** to serve as the macrocyclic precursor, which was synthesized through an *N*-methylation (of tyrosine **35** to form **36**) and peptide coupling sequence. Thus, the main hurdle was uncovering conditions best suited for the oxidative macrocyclization of the arylomycin core tripeptide. While nearly all conceivable oxidation methods explored were fruitless, copper-oxo complexes proved viable, and extensive optimization ultimately



led to a 60% yield on gram-scale. Development of this route dramatically increased access to supplies of the arylomycins and their analogs for academic research,<sup>40</sup> and the technology was ultimately licensed by Genentech for use in their ongoing drug discovery effort. While overall yield was dramatically increased and step count nearly cut in half, the ideality remains at 63%, **pointing mainly to the common shortcomings of peptide synthesis as discussed before.**

As part of a longstanding collaboration with LEO Pharma to pursue complex natural product synthesis in medicinal chemistry, the subglutinols became targets of interest due to their reported immunosuppressive activity (Figure 4).<sup>41</sup> Historically, such structures have been synthesized using purely polar-bond disconnections resulting in long sequences plagued by redox-manipulations and functional group interconversions.<sup>42</sup> Our strategy was guided by a desire to access as many members of the family as possible through a divergent approach enlisting a practical and scalable path to a common core followed by methods to controllably access the many substitution patterns and stereochemical configurations.<sup>43</sup> Modular, divergent approaches are always ideal in medicinal chemistry, and due to the diversity of methods for cross-coupling of differentially halogenated aromatic precursors, they are often straightforward to plan. Conversely, designing such an approach for a complex, stereochemically ornate natural product is uncommon. We began with the preparation of the key precursor **41** (from **40**) that represented the point of divergence, featuring an electrochemical variant of Snider's radical polycyclization.<sup>44</sup> After decarboxylative allylation, epoxidation and reduction could control the C-8 stereocenter in **42** (the opposite configuration was also accessed selectively). Following hydroboration/oxidation, the C-4 position was primed for use of a recently developed decarboxylative Giese reaction to set the C-4 stereocenter.<sup>45</sup> The C-12 center, in turn, could then be stereoselectively installed via a decarboxylative C-C alkenylation en route to **43** as employed in the syntheses of **29** and **34** (Figure 3).<sup>33</sup> The alternate stereoisomer could be accessed from the same intermediate by using a conventional Wittig/metathesis sequence. These radical methods were essential in simplifying this problem to reach not only **44** and three other members of the family but, in principle, a wide variety of analogs in a controlled fashion.<sup>42b,46</sup> Radical retrosynthesis, beyond canonical Stork-Curran type cyclizations, clearly offers unusual benefits to address the salient issues of this natural product class. **The less than perfect ideality (73%) is reflected in the need for vestigial PG manipulations and redox fluctuations to enable decarboxylative couplings and olefination.**

## 2019

The herquiline family of natural products, including herquiline C<sup>47</sup> (**49**), has intrigued and confounded the synthetic community since their first isolation by Omura in 1979 (Figure 4).<sup>48</sup> Centered on a [6.12.6.6] tetracyclic core, these strained alkaloid natural products possess an unusual reduced dityrosine cyclophane moiety. Successive NADH-mediated reductions are involved in the biosynthesis (from the parent dityrosine macrocycle); we therefore<sup>49</sup> sought to recapitulate Nature's direct and ideal strategy toward the herquelines in our own synthetic effort. Beginning from appropriately substituted iodotyrosines (**45** and **46**), a straightforward sequence rapidly led to the 12-membered macrocycle **47**,<sup>50</sup> setting the stage for the key reductive endgame. After testing every conceivable variable from reaction

conditions to order of operations, it was ultimately discovered that leveraging a Birch reduction on this highly strained macrocycle was a tractable solution. For the next reduction, Ir-catalyzed, silane mediated conditions were singularly effective in delivering the desired piperazine **48** in 86% yield on gram scale.<sup>51</sup> Ketalization of the vinyl methyl ether found in **48** proved pivotal to enable the final Birch reduction. This was presumably a consequence of the newly installed sp<sup>3</sup> center that both changed the conformation of the macrocycle and removed a problematic double bond prone to over-reduction. In using biosynthesis to guide the design, we were able to execute a simple and direct synthesis of the herquelines. In fact, apart from the necessary ketalization step, all maneuvers conducted en route to the natural product were strategic (87% ideality). That step is a reminder that **methods for chemo-selective arene reduction are still missing from the chemist's toolbox.**

Teleocidins<sup>52</sup> are bacterially produced,<sup>53</sup> potent inhibitors of protein-kinase-C activation<sup>54</sup> exhibiting a hybrid amino-acid/terpene based biosynthetic origin (Figure 4).<sup>55</sup> In Nature, these compounds are generated as a mixture of different isomers and reported synthetic routes have similarly led to mixtures of isomers.<sup>56</sup> This stems from the challenging problem of long-distance stereochemical relay across molecular architectures. A convergent strategy was devised wherein the indole-containing portion was formed first using chiral-pool derived building blocks and then fused using a catalytic stereoselective method to append the terpene portion. Commencing from 4-bromoindole (**50**), the valine subunit was appended through electrochemical amination using an amidine-based ligand to access **51**.<sup>57</sup> The C-3 tryptophol side chain was established through metalation and chiral aziridine ring opening. After macrolactamization and protection of the primary alcohol to form **52**, the stage was set to couple this fragment with a suitable polyunsaturated hydro-carbon after priming the C-6 position for coupling through C-H borylation.<sup>58</sup> With the boronic acid in hand after hydrolysis, application of Sigman's redox relay Heck reaction with homoallylic alcohol **53** cleanly forged the desired quaternary center in **54** with admirable control (6.6-7:1 d.r.).<sup>59</sup> Note that both isomers are found in the natural products, and simply changing the stereochemistry of the ligand delivered the opposite selectivity. The redox-economic nature of this powerful C-C bond forming method also prefaced the final ring closure, which was achieved via simple vinylolithium addition/Friedel-to generate a key Crafts alkylation sequence to provide **55**. Only modest control could be achieved in this final step as a function of the Brønsted acid employed. Of the 11 steps, 36% of them involved unfortunate protecting group manipulations due to **chemo-selectivity/reactivity requirements of the key skeletal bond forming reactions**. Finally, the C-H borylation may seem strategic and did indeed simplify the synthesis, but an even more direct approach would have been C-6 palladation followed by Heck to avoid the intermediate C-B bond that is not found in the target.

## 2020

Tryptorubin A<sup>60</sup> (**62**), isolated by Clardy in 2017,<sup>61</sup> is a peptidic macrocycle bearing a remarkable oxidatively fused skeleton wherein one tryptophan is interconnected with neighboring tyrosine and tryptophan residues through C-N and C-C linkages respectively, creating significant strain (Figure 5). Our motivation for pursuing **62** was based purely on



chemical curiosity as no bioactivity was reported for this family. The synthesis (starting with iodotyrosine **56**) was designed using a convergent strategy wherein an Ullman-derived<sup>62</sup> macrocyclic Ala-Trp-Tyr construct (**59**) could be coupled to a preoxidized Trp (pyrroloindoline)-Tyr (**60**) using Movassaghi's Friedel-Crafts arylation<sup>63</sup> to generate a key quaternary center. In practice, the natural product could only be obtained by using the indoline **59** rather than the indole **58**. After appending the final amino acid (Ile) to provide **61**, macrolactamization and reoxidation of the indoline to indole delivered **62** as a single isomer. At the outset, neither our group nor Clardy's team had any idea that this natural product could possibly exist as a different isomer. In fact, our original synthesis used intermediate **58** following a similar route to deliver an isomer of **62** whose identity was uncovered as the noncanonical atropisomer of **63**. For geometric reasons, the indoline oxidation state served to enforce the formation of only one isomer. Given the increased interest in complex macrocycles in drug discovery,<sup>64</sup> this kind of isomerism may be important to consider during the planning stages of synthesis and may be more widespread in natural product chemistry than previously appreciated. Had we carried out the initial synthesis with such a plan, this unusual type of isomerism in natural product chemistry may not have been uncovered. From an ideality standpoint this synthesis clearly suffers **from the challenges that plague most peptide syntheses: an overreliance on PG chemistry. In addition, the extraneous redox-fluctuation brought about by the indole-indoline-indole sequence clearly points to the difficulty in controlling planar chirality.**

Maximiscin<sup>65</sup> (**70**) is a natural product of mixed biosynthetic origin that results from the union of three separate metabolic pathways. The molecule exhibits unique structural features, including the peculiar linkage between the *N*-hydroxypyridone and polyketide-derived fragments that exists as a mixture of interconverting atropisomers (Figure 5).<sup>66</sup> This, along with its reported anticancer activity,<sup>67</sup> motivated our efforts to pursue its synthesis. A bold late-stage pyridone synthesis was envisaged to cleave the central ring and produce two equally sized fragments **67** and **69**. Application of radical retrosynthetic logic and the recognition of hidden symmetry via a desymmetrizing C-H activation allowed this highly convergent approach to begin from mesitylene-derived carboxylic acid **64** and shikimic acid **68**. These plans were rapidly put to practice through hydrogenation of **64** leading to a *meso* carboxylic acid that after a remarkable desymmetrizing C-H activation produced **65** whereby all *four* stereocenters of the saturated ring were simultaneously defined. Thereafter, directing group cleavage delivered a transient lactone, which was hydrolyzed and directly subjected to a decarboxylative homologation cascade. This carefully orchestrated step, proceeding in >90% yield (gram-scale) utilized a unique Ag/Fe cocatalyst system to both establish the hindered C-C bond with concomitant stereoinversion and effect tandem oxidation of the aldehyde via a 1,5-hydrogen atom transfer (HAT). Subsequently, Wittig olefination, sulfone oxidationalkylation, and acylation with Mander's reagent followed by *in situ* hydrolysis led to diacid **66**. The pivotal union of both fragments necessitated the use of reaction partners with enhanced reactivity: a trimethylsilyl-substituted oxime ether and a diacyl triflate electrophile generated *in situ*. This push-pull activation system ("aza-Sakurai") enabled the construction of the atropisomeric central pyridone ring and provided maximiscin in a 10-step LLS (60% ideality) after deprotection. While concise, common issues relating to C-H activations employing directing groups, a redox fluctuation resulting from a nonideal radical

acceptor, and deprotection of a polyol plagued 40% of the steps. **This highlights the need for further development of C- H activation methods directed by native functionality that obviate the need for directing group manipulations.**

Tagetitoxin<sup>68</sup> (**75**, Figure 5) is a complex alkaloid that has been of intense interest to the scientific community for nearly a century due to its controversial structural assignment (revised 3 times, absolute configuration and optical rotation unknown),<sup>69</sup> its collection of remarkable chemical features (fully oxidized cyclopentane core, multiple polar functional groups, more heteroatoms than carbon atoms), and unprecedented bioactivity (novel mechanism of RNA polymerase inhibition).<sup>70</sup> Motivated by those compelling attributes, our assembly of the fully oxidized cyclopentane core of tagetitoxin commenced from the commodity chemical furfural (**71**) via sulfonamide condensation followed by a Mannich-based amino ester synthesis and subsequent oxidative furan rearrangement to furnish **72** in high yield and diastereoselectivity. To install the chiral sulfide functionality, a thio-[3,3]-rearrangement of a suitably substituted allylic alcohol was executed through a sequence involving *p*-cyanobenzoyl protection, stereoselective Luche reduction, thio-CDI adduct formation, and heating followed by acidic hydrolysis to deliver **73** as a single diastereomer. A thio-Michael addition/catalytic dihydroxylation/bromocyclization sequence afforded the fully substituted bicycle **74**. To complete the synthesis of **75**, the key phosphate group was installed using the chiral P(V) reagent (+)-**Ψ**,<sup>71</sup> which was singularly successful in forging the key P-O bond and allowed for crystallization and divergent synthesis of each enantiomeric form of **75**. The accompanying concession steps were carefully planned deprotections necessitated by the extremely polar nature of **75** along with the oxidative removal (SeO<sub>2</sub>) of an extra sulfur atom from the **Ψ**-adduct. Employing an RNA polymerase assay on each enantiomer then allowed for assignment of (+)-**75** as the natural isolate. The low ideality of this 15-step route to **75** (60%) is unsurprising given the challenge of manipulating such a polar molecule. **This synthesis highlights the need for chemoselective methods that reduce reliance on PG manipulations and strategies for the late-stage incorporation of such functionality in their native form.**

## CONCLUSION

It is amazingly hard to find a simple solution. A complicated one is relatively easy.

Elon Musk

The progression of organic chemistry can be closely linked to increases in the simplicity and scalability of total syntheses during a given era, just as the age of a tree can be estimated by measuring its growth rings. For example, most skilled practitioners can examine a total synthesis and without knowing when it was published, roughly estimate the decade in which it was reported. New methods and strategies drive the evolution of synthesis to greater levels of ideality, which facilitates an objective and dispassionate analysis of how far we still have to go. This account chronicles the motivations for some of the molecules we have pursued over the past five years along with the sometimes-sobering lessons unearthed by aiming for the ideal synthesis. Several themes emerge from such an analysis that point to future directions in the field, some of which were highlighted above in bold. The syntheses of antroquinonol A,<sup>15</sup> pallambins,<sup>18</sup> and araiosamines<sup>25</sup> show how far the field has to go in

terms of site-selective C-C bond formation in molecules with only subtle electronic differences between functional groups. Herquelines,<sup>47</sup> tryptorubin A,<sup>60</sup> and cladospolides<sup>33</sup> remind us of the nonideal, yet often-employed, tactic of controlling selectivity through changes in oxidation state or temporary protection rather than through reagent/catalyst control. Maoecrystal V,<sup>20</sup> prostaglandins,<sup>33</sup> and subglutinols<sup>43</sup> used powerfully simplifying reactions for their rapid construction yet still suffered from superfluous redox changes that set the stage for such maneuvers. Lugdunin,<sup>27</sup> arylomycin,<sup>36</sup> tryptorubin A, and tagetitoxin<sup>68</sup> illuminate the reliance we still have on protecting group chemistry as a result of nonchemoselective reactions. Finally, teleocidins<sup>52</sup> and maximiscin<sup>65</sup> show the potential of C-H functionalization logic to simplify synthesis, even when those substrates require extra effort to install directing functionality. We also note that several of the syntheses above benefitted from a strategy of employing tandem one-pot sequences of mutually compatible reactions to further streamline routes. This is loosely analogous to biosynthesis where, for example, C-C bond formations, oxidations, and reductions can routinely happen in the same “vessel”. The continuous pursuit of mild and chemoselective methods will make such tandem sequences even more common.

Evaluating syntheses through the lens of ideality can pinpoint areas of methodology and strategy that can have the greatest impact in pushing the field forward. Over the decades to come, as the shortcomings delineated above drive solutions, the syntheses of this era will appear ancient; such an outcome can only happen through the hard work of continuous innovation and creative invention of the organic chemist.

## ACKNOWLEDGMENTS

The authors thank Scripps Research, the NIH (postdoctoral fellowship for C.R.P.), Bristol-Myers Squibb (graduate fellowships for D.S.P and K.S.M), and the NSF-GRFP (D.S.P) for their support.

**Funding** Financial support for the work included in this account was provided by Bristol-Myers-Squibb, LEO Pharmaceuticals, and the NIH/NIGMS (GM118176, GM-097444). Financial support in the form of fellowships for the contributors of the work included in this account was provided by NSF GRFP, NIH, the National Defense Science and Engineering Graduate Fellowship (NDSEG) Program, Bristol-Myers-Squibb, Vividion Therapeutics, Bayer Science, Nankai University, the ACS-MEDI Predoctoral Fellowship Program, the Swiss National Science Foundation, JSPS, the Honjo International Scholarship Program, Fujian Juhong Trade & Business Co., the George E. Hewitt Foundation, the German Research Foundation, the Tsinghua Xuetao Talent Program, and the Fulbright Scholar Program.

## Biographies

**David S. Peters** was born in San Francisco, CA, and received his B.A. in biochemistry from the University of San Diego. He is currently a graduate student in Prof. Baran’s laboratory pursuing the synthesis of antibacterial natural products.

**Cody Ross Pitts** is from Waterbury, CT. He obtained a B.S. in chemistry with minors in physics and musical theater from Monmouth University (2010), completed his Ph.D. at Johns Hopkins University (2011–2017), and conducted research abroad as an ETH Zürich postdoctoral fellow (2017–2019). Currently, he is an NIH postdoctoral fellow at Scripps Research.

**Kyle S. McClymont** was born in Ottawa, Canada, and received his B.Sc. and M.Sc. from the University of Ottawa. He then escaped the cold to complete a Ph.D. with Phil S. Baran at Scripps Research in La Jolla and currently works in discovery chemistry at Merck South San Francisco.

**Thomas P. Stratton** was born in Cranford, New Jersey, and received his B.A. in chemistry from Rutgers University-Newark. He subsequently pursued doctoral studies in the laboratory of Phil S. Baran at Scripps Research, studying alkaloid natural product syntheses. Following completion of his Ph.D., Tom joined the medicinal chemistry department at Gilead Sciences, Inc. He currently resides in San Francisco.

**Cheng Bi** was born in China and obtained his B.S. in Chemistry from Nankai University in 2018. He then joined Prof. Baran's laboratory as a graduate student focusing on natural product total synthesis.

**Phil S. Baran** completed his undergraduate education at New York University in 1997. After earning his Ph.D. at Scripps Research in 2001, he pursued postdoctoral studies at Harvard University until 2003, at which point he returned to TSRI to begin his independent career. He was promoted to the rank of professor in 2008 and is currently the Darlene Shiley Professor of Chemistry.

## REFERENCES

- (1). Newhouse T; Baran PS; Hoffmann RW The economies of synthesis. *Chem. Soc. Rev* 2009, 38, 3010. [PubMed: 19847337] The concepts of step, atom, and redox economy are discussed and contextualized with case studies.
- (2). Gaich T; Baran PS Aiming for the Ideal Synthesis. *J. Org. Chem* 2010, 75, 4657–4673. [PubMed: 20540516] A simple quantification of “ideality” in synthesis is presented alongside a self-evaluation of total syntheses from our laboratory over the seven years prior.
- (3). Kuttruff CA; Eastgate MD; Baran PS Natural product synthesis in the age of scalability. *Nat. Prod. Rep* 2014, 31, 419–432. [PubMed: 24337165] How the economies of synthesis can be leveraged to access natural products in a scalable fashion is analyzed herein.
- (4). Hendrickson JB Systematic synthesis design. IV. Numerical codification of construction reactions. *J. Am. Chem. Soc* 1975, 97, 5784–5800.
- (5). For a recent example of a 4-step total synthesis see: Zhuang Z; Herron A; Liu S; Yu J-Q Rapid Construction of Tetralin, Chromane, and Indane Motifs via Cyclative C-H/C-H Coupling: Four-Step Total Synthesis of (±)-Russujaponol F. *chemrxiv.org* 2020, DOI: 10.26434/chemrxiv.13250294.v1.
- (6). Wender PA; Verma VA; Paxton TJ; Pillow TH Function-Oriented Synthesis, Step Economy, and Drug Design. *Acc. Chem. Res* 2008, 41, 40–49. [PubMed: 18159936]
- (7). Trost B The atom economy—a search for synthetic efficiency. *Science* 1991, 254, 1471–1477. [PubMed: 1962206]
- (8). Burns NZ; Baran PS; Hoffmann RW Redox Economy in Organic Synthesis. *Angew. Chem., Int. Ed* 2009, 48, 2854–2867.
- (9). Bertz SH Convergence, molecular complexity, and synthetic analysis. *J. Am. Chem. Soc* 1982, 104, 5801–5803.
- (10). Hayashi Y Pot economy and one-pot synthesis. *Chem. Sci* 2016, 7, 866–880. [PubMed: 28791118]
- (11). Roschangar F; Zhou Y; Constable DJC; Colberg J; Dickson DP; Dunn PJ; Eastgate MD; Gallou F; Hayler JD; Koenig SG; Kopach ME; Leahy DK; Mergelsberg I; Scholz U; Smith AG; Henry M; Mulder J; Brandenburg J; Dehli JR; Fandrick DR; Fandrick KR; Gnad-Badouin F; Zerban G;

Groll K; Anastas PT; Sheldon RA; Senanayake CH Inspiring process innovation via an improved green manufacturing metric: iGAL. *Green Chem* 2018, 20, 2206–2211.

- (12). (a) Borovika A; Albrecht J; Li J; Wells AS; Briddell C; Dillon BR; Diorazio LJ; Gage JR; Gallou F; Koenig SG; Kopach ME; Leahy DK; Martinez I; Olbrich M; Piper JL; Roschangar F; Sherer EC; Eastgate MD The PMI Predictor app to enable green-by-design chemical synthesis. *Nat. Sustain* 2019, 2, 1034–1040. (b) Jimenez-Gonzalez C; Ponder CS; Broxterman QB; Manley JB Using the Right Green Yardstick: Why Process Mass Intensity Is Used in the Pharmaceutical Industry To Drive More Sustainable Processes. *Org. Process Res. Dev* 2011, 15, 912–917.
- (13). Ishihara Y; Montero A; Baran PS *The Portable Chemist's Consultant: A Survival Guide for Discovery, Process, and Radiolabeling*. Apple Publishing Group, 2013.
- (14). Kanda Y; Ishihara Y; Wilde NC; Baran PS Two-Phase Total Synthesis of Taxanes: Tactics and Strategies. *J. Org. Chem* 2020, 85, 10293–10320.
- (15). Villaume MT; Sella E; Saul G; Borzilleri RM; Fagnoli J; Johnston KA; Zhang H; Fereshteh MP; Dhar TGM; Baran PS Antroquinonol A: Scalable Synthesis and Preclinical Biology of a Phase 2 Drug Candidate. *ACS Cent. Sci* 2016, 2, 27–31. [PubMed: 27163023]
- (16). Lee T-H; Lee C-K; Tsou W-L; Liu S-Y; Kuo M-T; Wen W-C A New Cytotoxic Agent from Solid-State Fermented Mycelium of *Antrodia camphorata*. *Planta Med.* 2007, 73, 1412–1415. [PubMed: 17932820]
- (17). (a) Clinical Trials. <https://goldenbiotech.com/en/antroquinonol-hocena-clinical-trials-information/> (accessed 11/22/ 2020). (b) ClinicalTrials.gov Identifiers: NCT04523181, NCT03310632, NCT02047344, NCT02047344, NCT02047344, NCT02719028, NCT02719028, NCT04112147, NCT03622463, NCT04110873.
- (18). Martinez LP; Umemiya S; Wengryniuk SE; Baran PS 11-Step Total Synthesis of Pallambins C and D. *J. Am. Chem. Soc* 2016, 138, 7536–7539. [PubMed: 27284962]
- (19). Maezaki N; Gijzen HJM; Sun L-Q; Paquette LA Evaluation of Furan Photooxygenation as a Device for Construction of the Zaragozic Acid (Squalestatin) Core. *J. Org. Chem* 1996, 61, 6685–6692. [PubMed: 11667541]
- (20). Cernijenko A; Risgaard R; Baran PS 11-Step Total Synthesis of (–)-Maoecrystal V. *J. Am. Chem. Soc* 2016, 138, 9425–9428. [PubMed: 27457680]
- (21). Li S-H; Wang J; Niu X-M; Shen Y-H; Zhang H-J; Sun H-D; Li M-L; Tian Q-E; Lu Y; Cao P; Zheng Q-T Maoecrystal V, Cytotoxic Diterpenoid with a Novel C<sub>19</sub> Skeleton from *Isodon eriocalyx* (Dunn.) Hara. *Org. Lett* 2004, 6, 4327–4330. [PubMed: 15524475]
- (22). (a) Gong J; Lin G; Sun W; Li C-C; Yang Z Total Synthesis of (±) Maoecrystal V. *J. Am. Chem. Soc* 2010, 132, 16745–16746. [PubMed: 21049937] (b) Lu P; Gu Z; Zakarian A Total Synthesis of Maoecrystal V: Early-Stage C-H Functionalization and Lactone Assembly by Radical Cyclization. *J. Am. Chem. Soc* 2013, 135, 14552–14555. [PubMed: 24047444] (c) Peng F; Danishefsky SJ Total Synthesis of (±)-Maoecrystal V. *J. Am. Chem. Soc* 2012, 134, 18860–18867. [PubMed: 23126440] (d) Zhang W.-b.; Shao W.-b.; Li F.-z.; Gong J.-x.; Yang Z Asymmetric Total Synthesis of (–)-Maoecrystal V. *Chem. - Asian J* 2015, 10, 1874–1880. [PubMed: 26136342] (e) Zheng C; Dubovyk I; Lazarski KE; Thomson RJ Enantioselective Total Synthesis of (–)-Maoecrystal V. *J. Am. Chem. Soc* 2014, 136, 17750–17756. [PubMed: 25495370]
- (23). Han Q-B; Cheung S; Tai J; Qiao C-F; Song J-Z; Tso T-F; Sun H-D; Xu H-X Maoecrystal Z, a Cytotoxic Diterpene from *Isodon eriocalyx* with a Unique Skeleton. *Org. Lett* 2006, 8, 4727–4730. [PubMed: 17020288]
- (24). Seiple IB; Su S; Young IS; Nakamura A; Yamaguchi J; Jørgensen L; Rodriguez RA; O'Malley DP; Gaich T; Köck M; Baran PS Enantioselective Total Syntheses of (–)-Palau'amine, (–)-Axinellamines, and (–)-Massadines. *J. Am. Chem. Soc* 2011, 133, 14710–14726. [PubMed: 21861522]
- (25). Tian M; Yan M; Baran PS 11-Step Total Synthesis of Araisamines. *J. Am. Chem. Soc* 2016, 138, 14234–14237. [PubMed: 27748593]
- (26). Wei X; Henriksen NM; Skalicky JJ; Harper MK; Cheatham TE; Ireland CM; Van Wagoner RM Araisamines A–D: Tris-bromoindole Cyclic Guanidine Alkaloids from the Marine Sponge *Clathria (Thalysias) araiosa*. *J. Org. Chem* 2011, 76, 5515–5523. [PubMed: 21462976]

- (27). Malins LR; deGruyter JN; Robbins KJ; Scola PM; Eastgate MD; Ghadiri MR; Baran PS Peptide Macrocyclization Inspired by Non-Ribosomal Imine Natural Products. *J. Am. Chem. Soc* 2017, 139, 5233–5241. [PubMed: 28326777]
- (28). Becker JE; Moore RE; Moore BS Cloning, sequencing, and biochemical characterization of the nostocyclopeptide biosynthetic gene cluster: molecular basis for imine macrocyclization. *Gene* 2004, 325, 35–42. [PubMed: 14697508]
- (29). Zipperer A; Konnerth MC; Laux C; Berscheid A; Janek D; Weidenmaier C; Burian M; Schilling NA; Slavetinsky C; Marschal M; Willmann M; Kalbacher H; Schitteck B; Brötz-Oesterhelt H; Grond S; Peschel A; Krismer B Human commensals producing a novel antibiotic impair pathogen colonization. *Nature* 2016, 535, 511–516. [PubMed: 27466123]
- (30). Kricheldorf HR Polypeptides and 100 Years of Chemistry of  $\alpha$ -Amino Acid *N*-Carboxyanhydrides. *Angew. Chem., Int. Ed* 2006, 45, 5752–5784.
- (31). Si D; Sekar NM; Kaliappan KP A flexible and unified strategy for syntheses of cladospolides A, B, C, and iso-cladospolide B. *Org. Biomol. Chem* 2011, 9, 6988. [PubMed: 21850340]
- (32). Smith JM; Harwood SJ; Baran PS Radical Retrosynthesis. *Acc. Chem. Res* 2018, 51, 1807–1817. [PubMed: 30070821]
- (33). Edwards JT; Merchant RR; McClymont KS; Knouse KW; Qin T; Malins LR; Vokits B; Shaw SA; Bao D-H; Wei F-L; Zhou T; Eastgate MD; Baran PS Decarboxylative alkenylation. *Nature* 2017, 545, 213–218. [PubMed: 28424520]
- (34). Das S; Chandrasekhar S; Yadav JS; Grée R Recent Developments in the Synthesis of Prostaglandins and Analogues. *Chem. Rev* 2007, 107, 3286–3337. [PubMed: 17590055]
- (35). Corey EJ; Weinshenker NM; Schaaf TK; Huber W Stereo-controlled synthesis of di-prostaglandins F<sub>2</sub>. $\alpha$ . and E<sub>2</sub>. *J. Am. Chem. Soc* 1969, 91, 5675–5677. [PubMed: 5808505]
- (36). Peters DS; Romesberg FE; Baran PS Scalable Access to Arylomycins via C-H Functionalization Logic. *J. Am. Chem. Soc* 2018, 140, 2072–2075. [PubMed: 29381350]
- (37). (a)Roberts TC; Smith PA; Cirz RT; Romesberg FE Structural and initial biological analysis of synthetic arylomycin A<sub>2</sub>. *J. Am. Chem. Soc* 2007, 129, 15830–15838. [PubMed: 18052061]  
(b)Smith PA; Roberts TC; Romesberg FE Broad-spectrum antibiotic activity of the arylomycin natural products is masked by natural target mutations. *Chem. Biol* 2010, 17, 1223–1231. [PubMed: 21095572]
- (38). Smith PA; Koehler MFT; Girgis HS; Yan D; Chen Y; Chen Y; Crawford JJ; Durk MR; Higuchi RI; Kang J; Murray J; Paraselli P; Park S; Phung W; Quinn JG; Roberts TC; Rougé L; Schwarz JB; Skippington E; Wai J; Xu M; Yu Z; Zhang H; Tan M-W; Heise CE Optimized arylomycins are a new class of Gram-negative antibiotics. *Nature* 2018, 561, 189–194. [PubMed: 30209367]
- (39). Dufour J; Neuville L; Zhu J Intramolecular Suzuki-Miyaura Reaction for the Total Synthesis of Signal Peptidase Inhibitors, Arylomycins A<sub>2</sub> and B<sub>2</sub>. *Chem. - Eur. J* 2010, 16, 10523–10534. [PubMed: 20658499]
- (40). Walsh SI; Peters DS; Smith PA; Craney A; Dix MM; Cravatt BF; Romesberg FE The inhibition of protein secretion in *Escherichia coli* and sub-MIC effects of arylomycin antibiotics. *Antimicrob. Agents Chemother* 2019, 63, e01253–18. [PubMed: 30420476]
- (41). Lee JC; Lobkovsky E; Pliam NB; Strobel G; Clardy J Subglutinols A and B: Immunosuppressive compounds from the endophytic fungus *Fusarium subglutinans*. *J. Org. Chem* 1995, 60, 7076–7077.
- (42). (a)Kikuchi T; Mineta M; Ohtaka J; Matsumoto N; Katoh T Enantioselective Total Synthesis of (–)-Subglutinols A and B: Potential Immunosuppressive Agents Isolated from a Microorganism. *Eur. J. Org. Chem* 2011, 2011, 5020–5030.(b)Kim H; Baker JB; Lee S-U; Park Y; Bolduc KL; Park H-B; Dickens MG; Lee D-S; Kim Y; Kim SH; Hong J Stereoselective Synthesis and Osteogenic Activity of Subglutinols A and B. *J. Am. Chem. Soc* 2009, 131, 3192–3194. [PubMed: 19216570]
- (43). Merchant RR; Oberg KM; Lin Y; Novak AJE; Felding J; Baran PS Divergent Synthesis of Pyrone Diterpenes via Radical Cross Coupling. *J. Am. Chem. Soc* 2018, 140, 7462–7465. [PubMed: 29921130]
- (44). Snider BB Manganese(III)-Based Oxidative Free-Radical Cyclizations. *Chem. Rev* 1996, 96, 339–364. [PubMed: 11848756]



- (45). Qin T; Malins LR; Edwards JT; Merchant RR; Novak AJ; Zhong JZ; Mills RB; Yan M; Yuan C; Eastgate MD; Baran PS Nickel-Catalyzed Barton Decarboxylation and Giese Reactions: A Practical Take on Classic Transforms. *Angew. Chem., Int. Ed* 2017, 56, 260–265.
- (46). Zhang F; Danishefsky SJ An Efficient Stereoselective Total Synthesis of dl-Sesquicillin, a Glucocorticoid Antagonist. *Angew. Chem., Int. Ed* 2002, 41, 1434–1437.
- (47). He C; Stratton TP; Baran PS Concise Total Synthesis of Herquines B and C. *J. Am. Chem. Soc* 2019, 141, 29–32. [PubMed: 30575396]
- (48). Enomoto Y; Shiomi K; Hayashi M; Masuma R; Kawakubo T; Tomosawa K; Iwai Y; Omura S Herquiline B, a New Platelet Aggregation Inhibitor Produced by *Penicillium herquei* Fg-372. *J. Antibiot* 1996, 49, 50–53.
- (49). Yu X; Liu F; Zou Y; Tang M-C; Hang L; Houk KN; Tang Y Biosynthesis of Strained Piperazine Alkaloids: Uncovering the Concise Pathway of Herquiline A. *J. Am. Chem. Soc* 2016, 138, 13529–13532. [PubMed: 27690412]
- (50). Zhu X; McAtee CC; Schindler CS Scalable Synthesis of Mycocyclusin. *Org. Lett* 2018, 20, 2862–2866. [PubMed: 29701978]
- (51). Cheng C; Brookhart M Iridium-Catalyzed Reduction of Secondary Amides to Secondary Amines and Imines by Diethylsilane. *J. Am. Chem. Soc* 2012, 134, 11304–11307. [PubMed: 22770123]
- (52). Nakamura H; Yasui K; Kanda Y; Baran PS 11-Step Total Synthesis of Teleocidins B-1-B-4. *J. Am. Chem. Soc* 2019, 141, 1494–1497. [PubMed: 30636411]
- (53). Takashima M; Sakai H A New Toxic Substance, Teleocidin, Produced by *Streptomyces*. *Bull. Agric. Chem. Soc. Jpn* 1960, 24, 647–655.
- (54). Umezawa K; Weinstein IB; Horowitz A; Fujiki H; Matsushima T; Sugimura T Similarity of teleocidin B and phorbol ester tumour promoters in effects on membrane receptors. *Nature* 1981, 290, 411–413. [PubMed: 6261139]
- (55). Awakawa T; Abe I Biosynthesis of the teleocidin-type terpenoid indole alkaloids. *Org. Biomol. Chem* 2018, 16, 4746–4752. [PubMed: 29774913]
- (56). (a) Nakatsuka S.-i.; Masuda T; Goto T Total syntheses of (±)-teleocidin B-3 and B-4. *Tetrahedron Lett* 1987, 28, 3671–3674. (b) Okabe K; Muratake H; Natsume M Synthesis of teleocidins A, B and their congeners. Part 3. Synthesis of dihydroteleocidin B-4 (dihydroteleocidin B), teleocidin B-3 and teleocidin B-4. *Tetrahedron* 1991, 47, 8559–8572.
- (57). Li C; Kawamata Y; Nakamura H; Vantourout JC; Liu Z; Hou Q; Bao D; Starr JT; Chen J; Yan M; Baran PS Electrochemically Enabled, Nickel-Catalyzed Amination. *Angew. Chem., Int. Ed* 2017, 56, 13088–13093.
- (58). Feng Y; Holte D; Zoller J; Umemiya S; Simke LR; Baran PS Total Synthesis of Verruculogen and Fumitremogin A Enabled by Ligand-Controlled C-H Borylation. *J. Am. Chem. Soc* 2015, 137, 10160–10163. [PubMed: 26256033]
- (59). Mei T-S; Patel HH; Sigman MS Enantioselective construction of remote quaternary stereocentres. *Nature* 2014, 508, 340–344. [PubMed: 24717439]
- (60). Reisberg SH; Gao Y; Walker AS; Helfrich EJN; Clardy J; Baran PS Total synthesis reveals atypical atropisomerism in a small-molecule natural product, tryptorubin A. *Science* 2020, 367, 458–463. [PubMed: 31896661]
- (61). Wyche TP; Ruzzini AC; Schwab L; Currie CR; Clardy J Tryptorubin A: A Polycyclic Peptide from a Fungus-Derived Streptomyces. *J. Am. Chem. Soc* 2017, 139, 12899–12902. [PubMed: 28853867]
- (62). Kunz K; Scholz U; Ganzer D Renaissance of Ullmann and Goldberg Reactions - Progress in Copper Catalyzed C-N-, C-O- and C-S-Coupling. *Synlett* 2003, 2428–2439.
- (63). Kim J; Movassaghi M Concise Total Synthesis and Stereochemical Revision of (+)-Naseseazines A and B: Regioselective Arylative Dimerization of Diketopiperazine Alkaloids. *J. Am. Chem. Soc* 2011, 133, 14940–14943. [PubMed: 21875056]
- (64). (a) Cummings MD; Sekharan S Structure-Based Macrocyclic Design in Small-Molecule Drug Discovery and Simple Metrics To Identify Opportunities for Macrocyclization of Small-Molecule Ligands. *J. Med. Chem* 2019, 62, 6843–6853. [PubMed: 30860377] (b) Driggers EM; Hale SP; Lee J; Terrett NK The exploration of macrocycles for drug discovery — an underexploited structural class. *Nat. Rev. Drug Discovery* 2008, 7, 608–624. [PubMed: 18591981]

- (65). McClymont KS; Wang F-Y; Minakar A; Baran PS Total Synthesis of (–)-Maximiscin. *J. Am. Chem. Soc* 2020, 142, 8608–8613. [PubMed: 32338003]
- (66). Du L; Robles AJ; King JB; Powell DR; Miller AN; Mooberry SL; Cichewicz RH Crowdsourcing Natural Products Discovery to Access Uncharted Dimensions of Fungal Metabolite Diversity. *Angew. Chem., Int. Ed* 2014, 53, 804–809.
- (67). Robles AJ; Du L; Cichewicz RH; Mooberry SL Maximiscin Induces DNA Damage, Activates DNA Damage Response Pathways, and Has Selective Cytotoxic Activity against a Subtype of Triple-Negative Breast Cancer. *J. Nat. Prod* 2016, 79, 1822–1827. [PubMed: 27310425]
- (68). He C; Chu H; Stratton TP; Kossler D; Eberle KJ; Flood DT; Baran PS Total Synthesis of Tagetitoxin. *J. Am. Chem. Soc* 2020, 142, 13683–13688. [PubMed: 32687336]
- (69). Aliev AE; Karu K; Mitchell RE; Porter MJ The structure of tagetitoxin. *Org. Biomol. Chem* 2016, 14, 238–245. [PubMed: 26517805]
- (70). (a) Mathews DE; Durbin RD Tagetitoxin inhibits RNA synthesis directed by RNA polymerases from chloroplasts and *Escherichia coli*. *J. Biol. Chem* 1990, 265, 493–498. [PubMed: 1688434] (b) Vassilyev DG; Svetlov V; Vassilyeva MN; Perederina A; Igarashi N; Matsugaki N; Wakatsuki S; Artsimovitch I Structural basis for transcription inhibition by tagetitoxin. *Nat. Struct. Mol. Biol* 2005, 12, 1086–1093. [PubMed: 16273103] (c) Yuzenkova Y; Roghanian M; Bochkareva A; Zenkin N Tagetitoxin inhibits transcription by stabilizing pretranslocated state of the elongation complex. *Nucleic Acids Res.* 2013, 41, 9257–9265. [PubMed: 23935117]
- (71). Knouse KW; deGruyter JN; Schmidt MA; Zheng B; Vantourout JC; Kingston C; Mercer SE; McDonald IM; Olson RE; Zhu Y; Hang C; Zhu J; Yuan C; Wang Q; Park P; Eastgate MD; Baran PS Unlocking P(V): Reagents for chiral phosphor-othioate synthesis. *Science* 2018, 361, 1234–1238. [PubMed: 30072577]

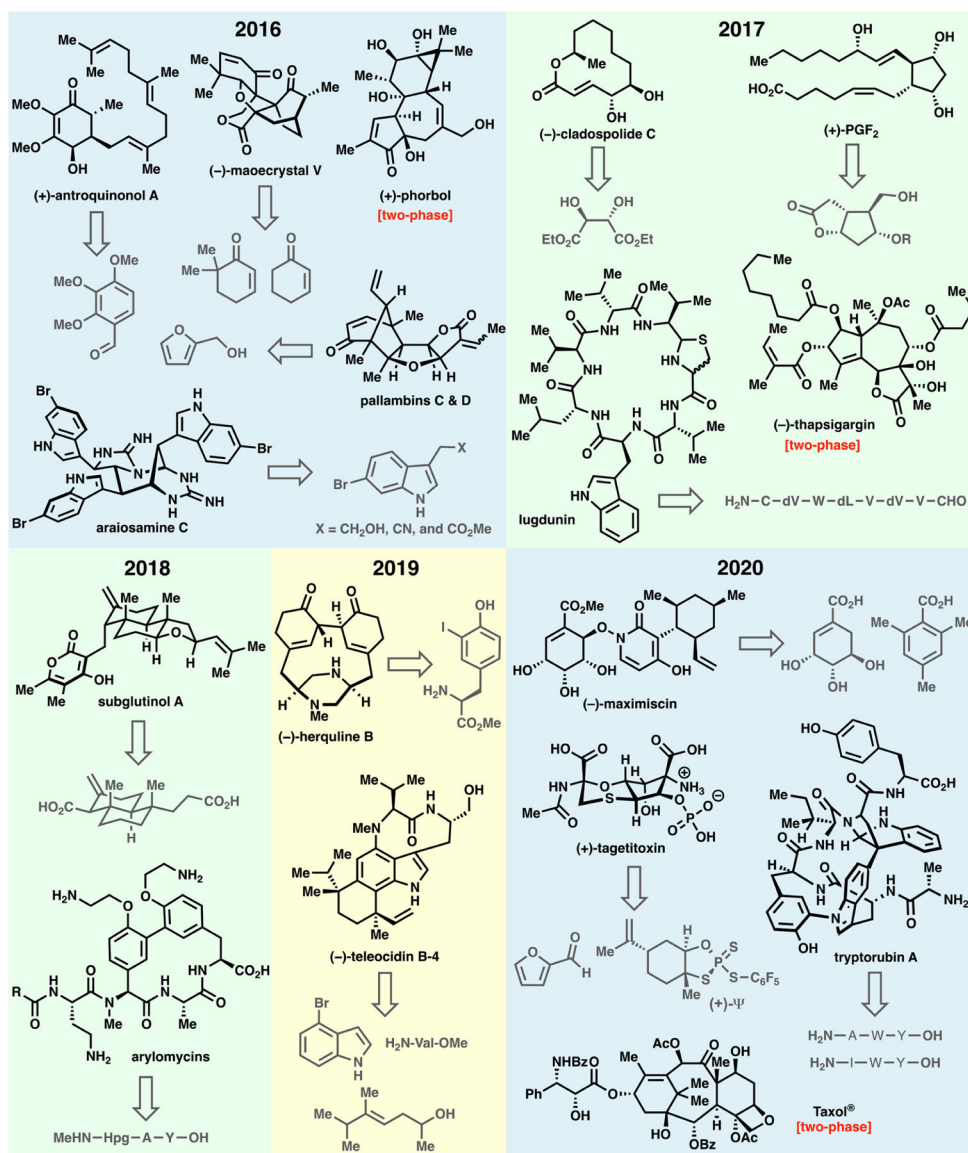


**Figure 1.**  
Select molecules synthesized in our laboratory over the past five years.

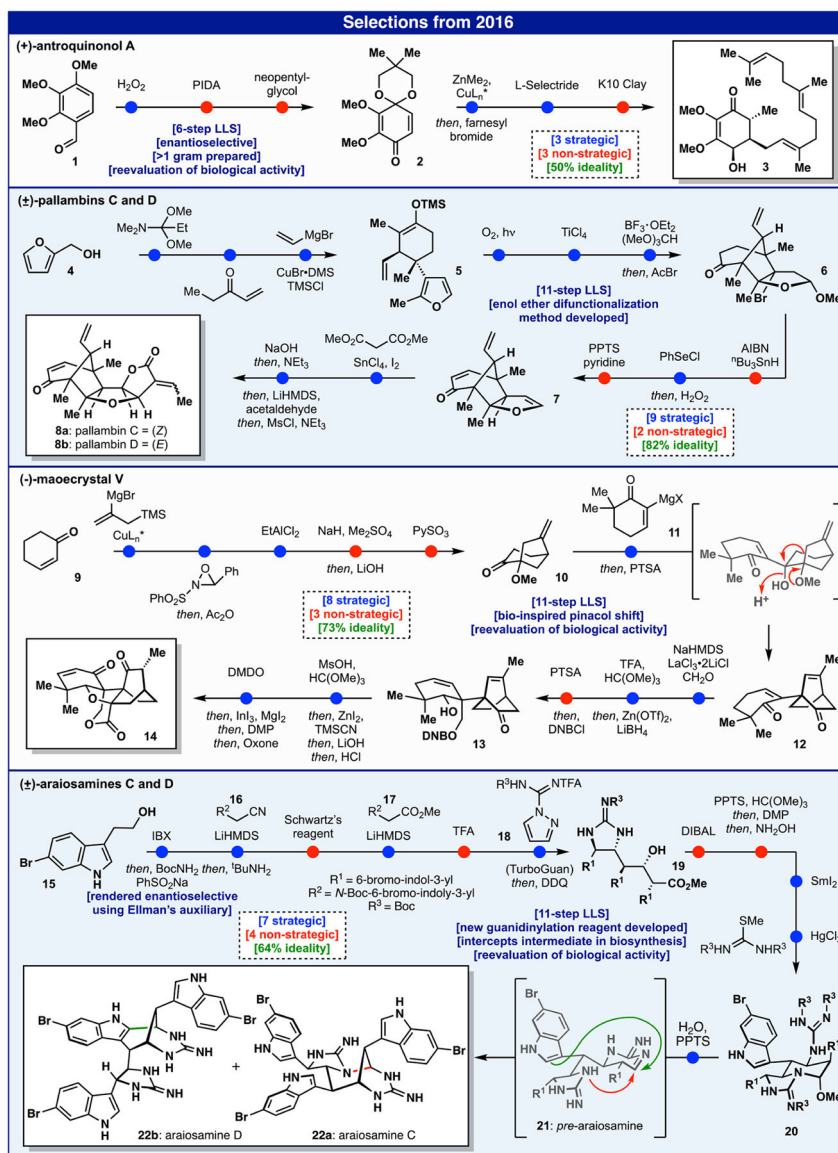


**Figure 2.**  
 Select total syntheses from 2016.

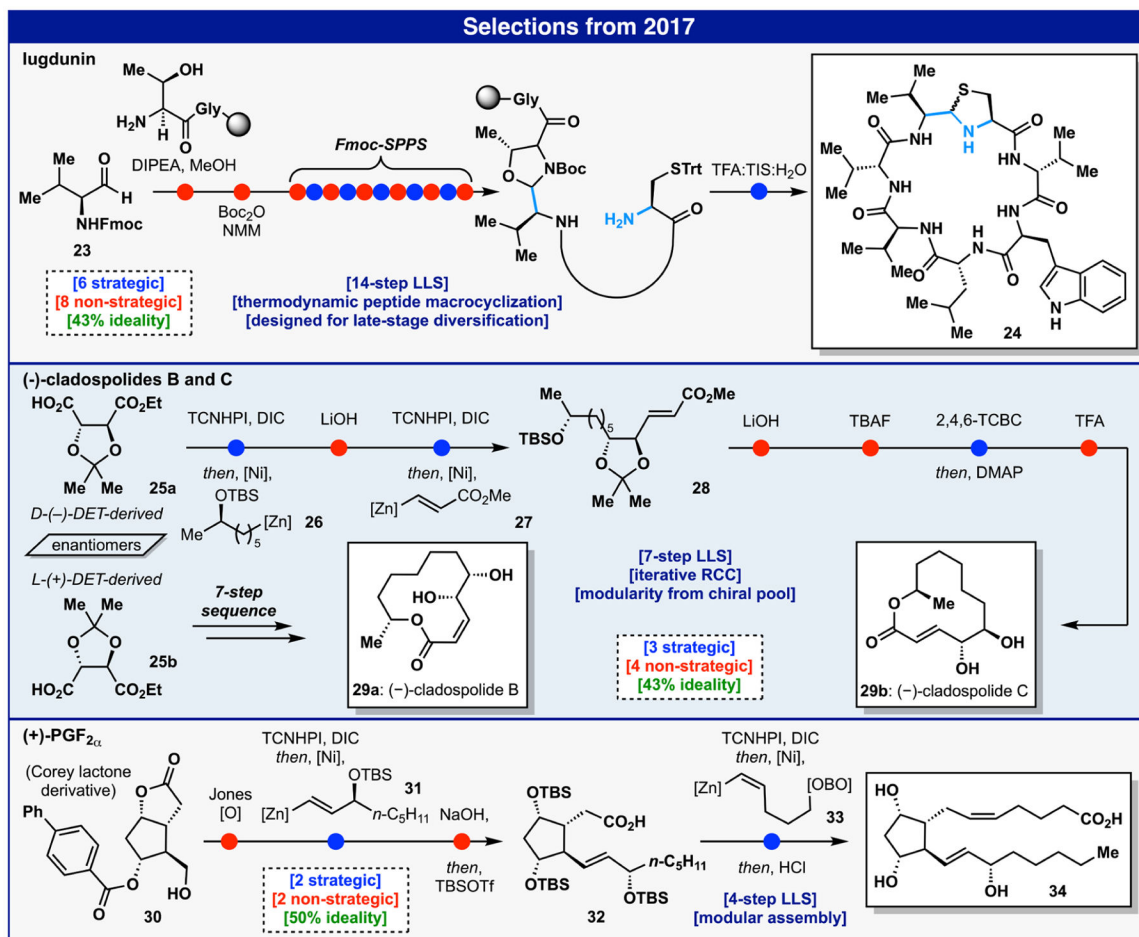


**Figure 3.** Select total syntheses from 2017; TCNHPI = tetrachloro-*N*-hydroxyphthalimide.





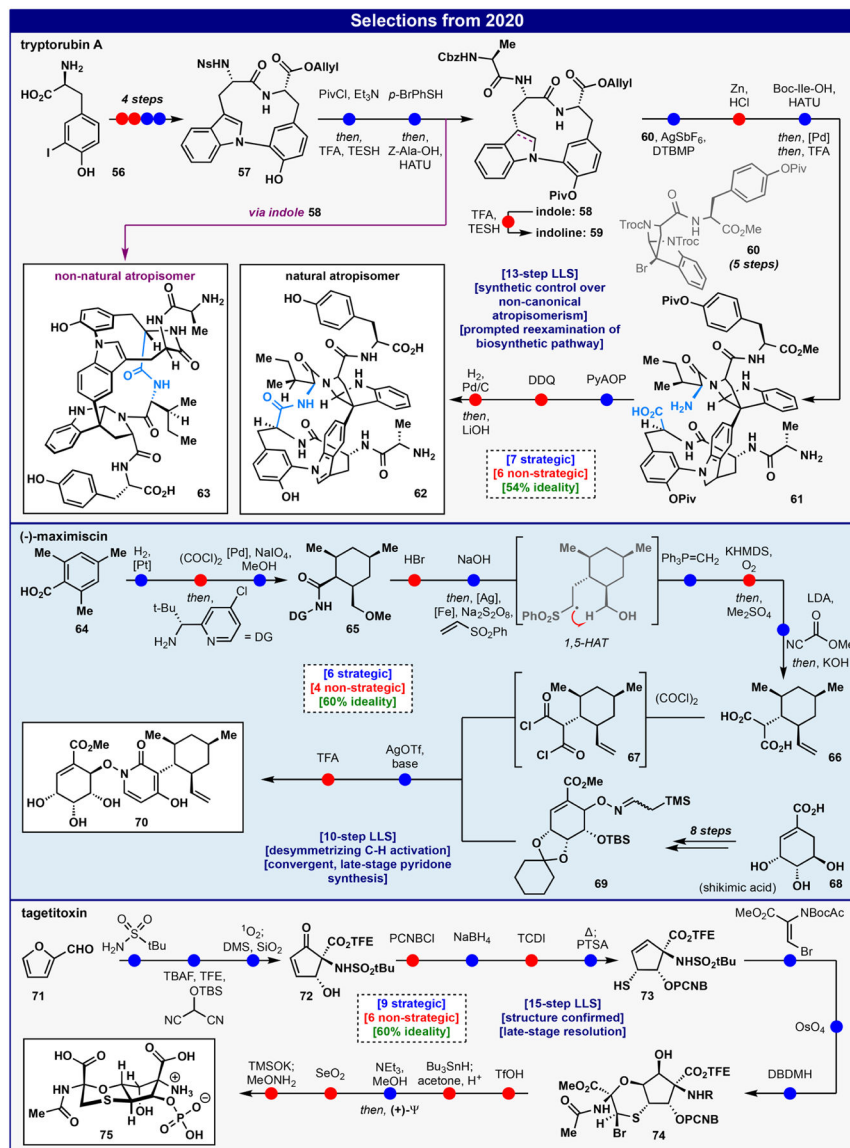


**Figure 5.**  
Select total syntheses from 2020.